Al-Sibd Center for Research and Scholarly Publishing
Iraqi Journal of Nanotechnology
synthesis and application
Journal Homepage : https://publications.srp-center.iq/index.php/ijn

Novel Applications Using Magnetron Sputtering and Atmospheric-Pressure Plasma Jet Techniques: A Review

Ahmed Abed Anber[1*], Jafer Fahdel Odah[2], Mazin Mohammed Mawat[3]

[1*] Department of Renewable Energy Science, College of Energy and Environment Science, AL Karkh University of Science, Baghdad, Iraq
[2] Department of Medical Physics, College of Science, AL-Karkh University of Science, Baghdad, Iraq
[3] College of Medicine, Wasit University, Wasit, Iraq

*Corresponding author: Email address: ahmedkrm88@gmail.com

Keywords:
Magnetron sputtering;
Atmospheric-pressure plasma jet;
Phases of copper oxide nanostructures.

Abstract

Nanomaterials are now widely used in a variety of fields, such as biomedicine and industry, and the world is experiencing its worst conditions yet as a result of the spread of bacteria and the rise in the number of people infected with various diseases as a result of coming into contact with nanomaterials. The spread of pollution can be curtailed by the use of new techniques and experiments. Microorganism membranes can be penetrated by nanoparticles, making nanostructured materials a necessity in biological research. The plasma jet technology is powerful enough to sterilize and kill the bacteria in a small space. There are a wide variety of industrially essential coatings that Magnetron sputtering can be applied to, including those used in the medical industry. We'll go over the history, foundation, and several uses of this method in this review. Other recent discoveries, such as the creation of copper oxide nanoparticles in each of the two processes, are also covered. It can be used in a variety of fields, including biomedical applications. Nanoparticles of copper oxide have the potential to sterilize and kill microorganisms, making them a crucial medical tool to have on hand.

Introduction

The magnetron configuration is one of the applications for developing the method of coating, it can modify the power of electrodes cathode and anode to get a product. Sputtering is a very important technique particularly when it comes to the magnetic field (magnetron). The effect of magnetic field confinement onto electrodes gained many acceptable results [3-7]. The electrode (anode) is located vertically on cathode to let the substrate bombardment appear with high power. The physical sputtering combination and all reactions on the surface of target in a plasma environment is termed reactive plasma sputtering. As a consequence of different parameters, some explanations can be

©SRP 2023, DOI: https://doi.org/10.47758/ijn.vi4.98

workable [8, 9]. Via sources (one or two) like metals, semiconductors or insulators in Ar/O_2 or extra effective gases for deposition drives are frequently selected to rise the sputtering yield with respect to the components of chemical structure that can be resumed [10]. The yield of sputtering indicates to get a good films homogeneity and refer to low-cost production, particularly with gases reactive in magnetron plasma sputtering. In fact, the cathode and anode will act together depending on the addition of a gases that have many reactive features. The target of potential in the sputter yield atoms form the target will be increase. The feature for producing the breakdown voltage of distance "pd" and pressure is very important, however it has little reliability on the electrode material that defines the secondary electrons and an electric field is recognized linearly with pressure ($E = V/d$) [11]. Thus, the minimum *p.d* in the Paschen's curve represents the minimum value of break down voltage that is equal to generate the gas discharge *p.d*:

$$pd\big|_{V_{\min}} = \frac{1}{A}\log\left(1+\frac{1}{\gamma_e}\right)$$

While the value of pressure and distance between two electrodes is exactly huge, the ions released in the gases are decelerated due to serious collisions therefore, it will hit the target via way of energy to generate emission of secondary electrons. Commonly sputtering discharges voltage is comparatively enormous. The number of ions increase because the collision with atoms of gases will increase also [11]. Whole ions are coming back to the electrode and delivers many electrons. The gases will current and voltage will drop, then current value will increase gradually [12]. Additionally, the secondary electrons of the material are 0.1., and one ion will smash the region of the electrode (cathode) to discharge the secondary electron. Therefore, the region of normal glow that observers the electrode bombardment will help the surface of electrode establish the mechanism of sputtering. At first, the bombardment is not humongous. Normally, the bombardment increases the shield when the power is accessible; the electrode surfaces up until the current density (*J*) is understood [13]. Subsequently, the voltage V and *J* in discharge increase when power produces also increase [14]. If the target is un-cooled, both of thermal and secondary electrons are emitted when the value of (*J*) current density about ($0.1 A/cm^2$). It relies on the average of mean free path distance between the two electrodes also the emission of secondary electrons. Each electron needs from 10 to 20 ions for the novel avalanche to stand up. The secondary electrons cannot undertake passable number of collisions ion to hit the electrode anode [15]. Also, Kelly and Arnell have defined the dark space [16-17]. The electrons are accelerated from the cathode to anode which are caused to collide with ions [18]. Because of the variations from its fabrication process, cuprous oxide (Cu_2O) is a p-type semiconductor with varied optical properties. [19]. copper oxide: Cu_2O and CuO, known as (cupric oxide), have been grown using a variety of techniques [18-19]. Additionally, the energy gaps for (Cu_2O) molecule [6–13], as well as (CuO) molecule [10–13] films, which have been reported in literature, rely on a manufacturing procedure Energy gap values for (Cu_2O) molecule range (2.10-2.60) eV [6-13], whereas CuO has been reported to have an energy gap of 1.3-2.1 eV [10, 13]. Films made of Cu_2O absorb light at wavelengths as short as 600 nm, whereas films made of CuO absorb light across the whole visible spectrum [19]. Moreover, copper oxide films are used in many other applications. A band gap energy values of copper oxide films have been reported to be suitable for utilization as solar energy conversion windows [20]. Spectrally selective variable reflectance coatings based on copper oxide films have been demonstrated by Richardson in architectural applications. Requirements for solar cell windows include transparency in the visible spectrum and low electrical resistance ($\rho_{electrical}$). Despite of its requirements, CuO has large value of electrical resistivity ($\rho_{electrical}$). The range of resistivity from 102 to 104 Ohm cm, are prepared by thermal preparation methods and no much difference in electro-deposition method which is around (104 -106 Ohm cm)

©SRP 2023, DOI: https://doi.org/10.47758/ijn.vi4.98

[15]. Many efforts were prepared in works to fabricate copper oxide Cu_2O nanostructure with small ($\rho_{electrical}$). Many researchers [14,15] have been struggling to synthesize copper oxide nanostructures via magnetron sputtering, which had the potential to yield a range of copper oxide nanostructure films with stoichiometry changing from rich copper to Cu_2O nanostructures and lastly (CuO) via varying the parameters in the plasma sputtering system. Copper oxide nanostructure films was prepared by direct current DC, radio frequency RF and reactive sputtering, it could change the resistivity of the prepared nanostructure films by controlling in the oxygen ratio (pressure of O_2). CuO nanostructure films with resistivity as low as 25 Ohm cm and the output power was 200 watts in the plasma sputtering system. Truthfully, this review purposes to characterize plasma magnetron sputtering technique and optimize the magnetron configuration with operation conditions to study the preparation of different molecular phases of copper oxide thin films and nanostructures at optimum conditions. The plasma jet technique represents one of the best it has huge utility because of its features, [19-20]. The atmospheric pressure plasma jets a good optimum for numerous applications, like surface modification, medical treatment and nanoparticles [21]. The characterization of plasma provides the limitless prospective to study the biomedical applications. These techniques are used to kill and treat diseases (virus and bacteria) and decontaminate and remove cells without affecting necrosis to treat cells [21]. Additionally, it has a simple design. The cathode (high-voltage electrode) is commonly made from a needle syringe with metal pin or the use of a glass needle. Biomedical applications should be adjacent room temperature and takes a short current when the system of plasma was used. The discharge gas flows over the pin at a different flow rate and uses the controller to regulate the gas flow rate [21]. The application, like cancer treatment sterilization, bleaching (dentistry), and healing of wound treatment have been demonstrated [22]. It is important to know the parameters of plasma-like electron temperature and density of electron. To obtain these parameters at low-pressure plasma, this microorganism produces some enzymes which are associated with the pathogenesis of *P. Aeruginosa* infections. In spite of the developments in antibiotic treatment, *P. Aeruginosa* is basically resistant to a number of that antibiotic [23]. Cold plasma can support as an alternative to other conventional decontamination methods like heat, chemical, and irradiation sterilization methods, especially for sterilizing heat-sensitive tools. It encourages an effective killing/sterilizing of the microbes and decreases the pollution [24].

Synthesis of CuO and Ag Nanostructures

The highest components of home-made reactive magnetron sputtering system is shown in Figure 1. Two magnetrons at the cathode and anode electrodes were verified.

©SRP 2023, DOI: https://doi.org/10.47758/ijn.vi4.98

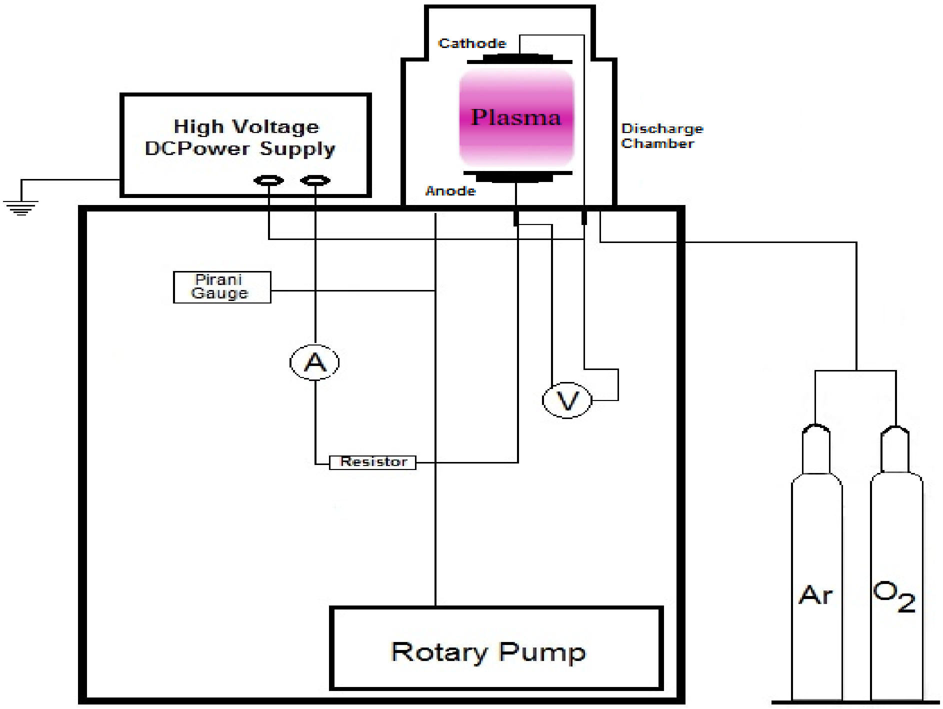

Figure 1. The schematic diagram of sputtering system

The design of electrodes was shown in Fig. 2. The cathode and anode are made of copper; and the thickness of diameter for each disc is (6 cm and 3 mm), respectively. The concentric magnets have been put behind each cathode and anode to create the magnetron fields. Also, the inner and outer diameters of the magnets are 2 and 5 cm, respectively. Both electrodes have been combined to power supply (direct current) to make power available for discharge. The anode was fixed perpendicularly as the electrode (anode), while the cathode was the moved upper electrode and the spacing of two electrodes were prepared (1- 6) cm.

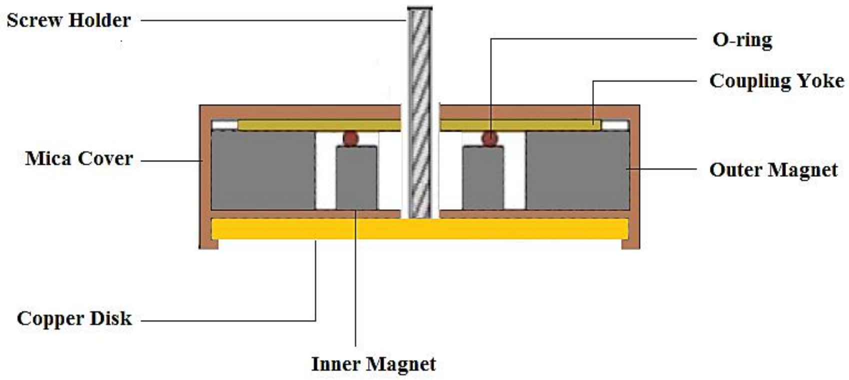

Figure 2. The discharge electrode design

©SRP 2023, DOI: https://doi.org/10.47758/ijn.vi4.98

Paschen's curve of Ar gas with magnetrons of different inter-electrode distance (from 2 to 4.5cm) have been shown in Fig. 3. The curves are shifting to higher breakdown voltages, with the increase of inter-electrode distance. When the pressure is low, the electrons must have more energy to complete the ionization of neutral atoms [21].

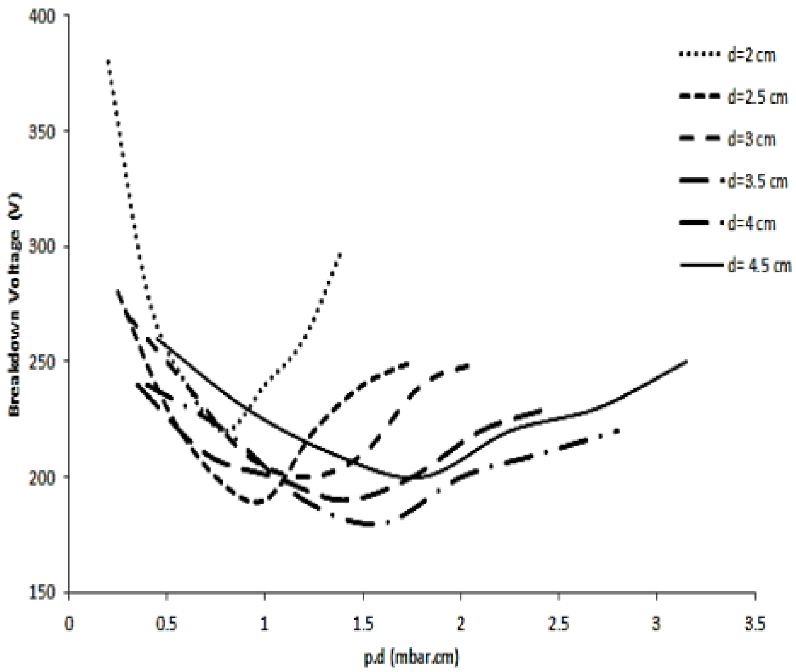

Figure 3. Paschen curves at different inter-electrode distance using Ar gas discharge [21].

Figure 4 shows the magnetic field intensity. The top value was observed at inter-electrode distance 4.5 cm, while the lowest value was at inter-electrode distance 2 cm. The probe diameter stayed around (0.8 cm). The interfering between magnetic field lines and high interfering occurred at the midpoint of distance of (2 cm). When the distance between electrodes reaches the “no interference” conditions at inter-electrode distance ≥ 5 cm the acceleration of electrons via electric and magnetic fields has more drift velocities then the probe might not attract from their paths between two electrodes [21].

©SRP 2023, DOI: https://doi.org/10.47758/ijn.vi4.98

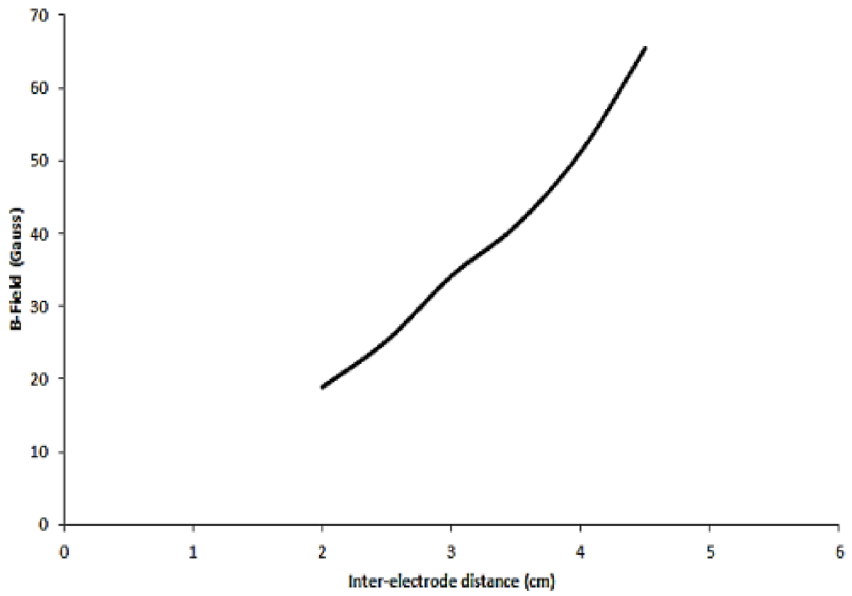

Figure 4. The magnetic field intensity (B-field) with inter-electrode distance (d) [21].

Preparing CuO requires a direct current reactive dual magnetron sputtering. The target (cathode) was made of high pure copper disk (99.999%). The nanostructured oxide films have been produced in an Argon: Oxygen gases. The substrates, which are made of glass, were cleaned before being placed inside the discharge chamber. The total gas pressure was $5*10^{-2}$ mbar., and inter-electrode distance was 2.5 cm with controlling to ratio of Argon: Oxygen gases, are between 1:1 and 2:1. Conversely, two phases cupric (CuO) and corpus (Cu_2O) have been produced. The discharge current was 300 milliampere while the discharge voltage could be accurately changed from 0 to 2000 volt. The deposition rate took about 5-8 minutes to obtain dark films of copper oxide CuO. To get more crystallinity and obtain a new phase of copper oxide Cu_2O, the samples films of CuO have been annealed at 450 C^o and the time was 2 hours to gain high homogeneity in the structures. XRD examination and (FTIR) Fourier transforms infrared spectroscopy model Shimadzu 8400S, were used to characterize the samples of copper oxide nanostructure films. The samples in gas sensing applications were examined at various temperatures and with various gases using a home-made apparatus. For the XRD patterns of pure phase Cu_2O and CuO at 2*10-2 mbar with Argon: Oxygen 1:1 and 1:2 gas mixing rates, respectively, as shown in Figure 3. Cupric oxide phases and cuprous oxide peak characteristics match those of the samples' peaks. CuO nanostructures may be seen as two peaks at 2ϴ 38.18° and 38.57° with (hkl) values (111) and (110). At 2 of 29.52 degrees, there are four peaks with (hkl) of (110), (111) and (200) that suggest the presence of Cu_2O. It is conceivable that the increased crystallinity of copper oxide results from an increase in oxygen ratios [24,25].

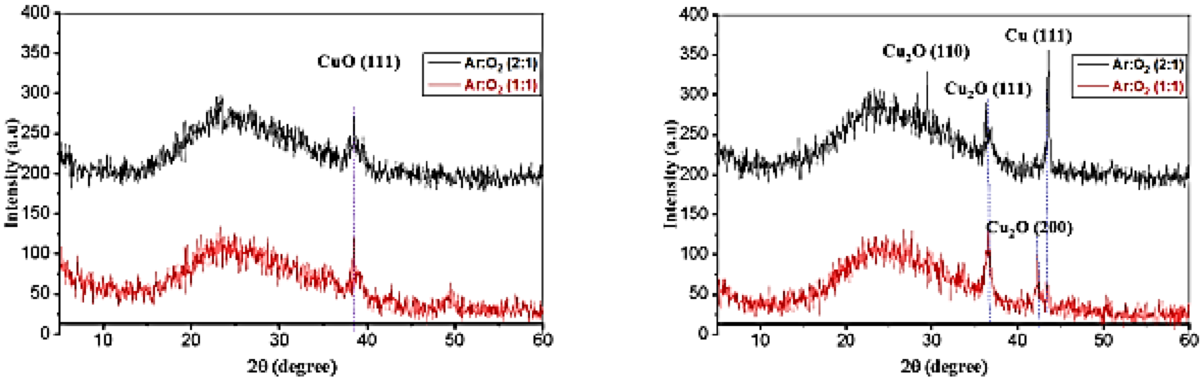

Figure 5: Radiation analysis, specifically X-ray diffractograms Using the magnetron sputtering process, patterns of CuO films were created at a distance of (d= 2.5 cm) without any heat treatment. Heat-treated Cu2O films at (2.5 cm) between electrodes after magnetron sputtering at 450 Co for 2 hours were analyzed using the XRD technique.[20]

This review has shown the phase of CuO and Cu_2O thin films prepared via a dual magnetron sputtering technique at inter-electrode distance of 2.5 cm with mixing ratios of Argon: Oxygen gases without and with annealing, and achieving these samples as a gas sensor application. It is very important to study the degree of gas sensitivity through NO_2 and NH_3 gases. The sensitivity to NO_2 gases is upper than sensitivity to NH_3 gases, according to the results of the experiment. It was very important to detect the toxic gas leak in hospitals and laboratory.

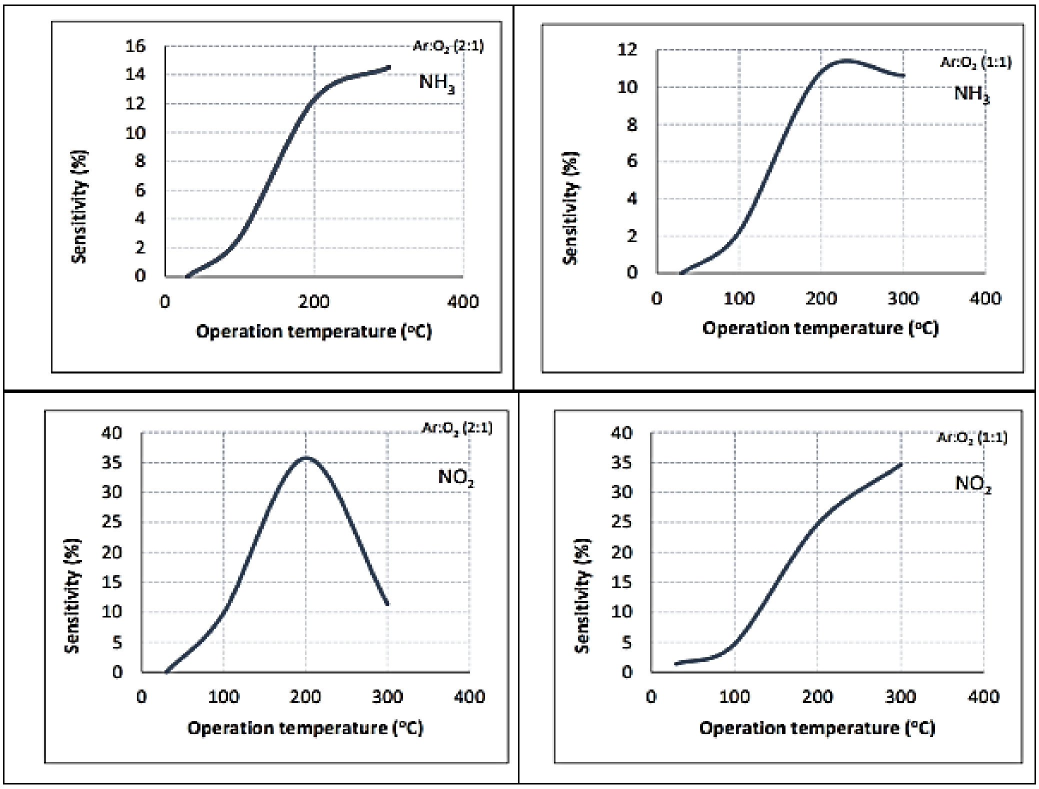

a

Figure 6-a Time-dependent sensitivities of CuO nanostructure films produced by using dual magnetron sputtering and 2.5cm inter-electrode spacing in NH_3 and N_2, respectively, without or with heat treatment. [20].

©SRP 2023, DOI: https://doi.org/10.47758/ijn.vi4.98

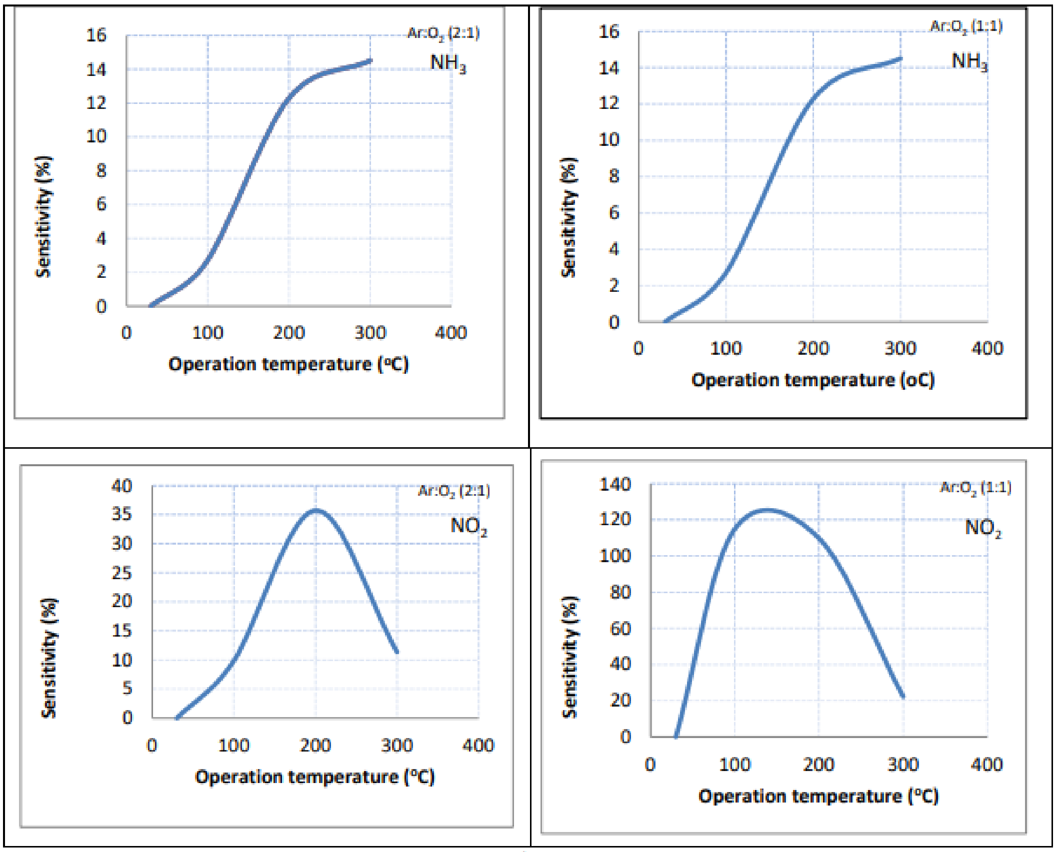

Figure 6-b Effect of working time on the sensitivities of dual magnetron sputtering-produced Cu2O films, measured with and without heat treatment of NO_2 and NH_3 gas at a 2.5cm inter-electrode distance. [20].

figure 7 and figure 8 display synthesizing by atmospheric-pressure plasma jet for copper oxide nanoparticles CuO and the experimental system [22], where the polycrystalline structure has been referred.

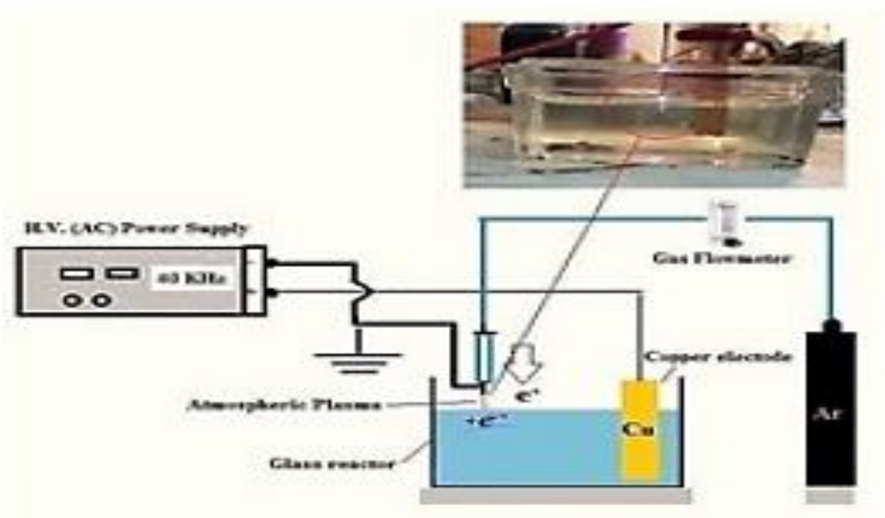

Figure 7 The atmospheric-pressure plasma jet [21].

©SRP 2023, DOI: https://doi.org/10.47758/ijn.vi4.98

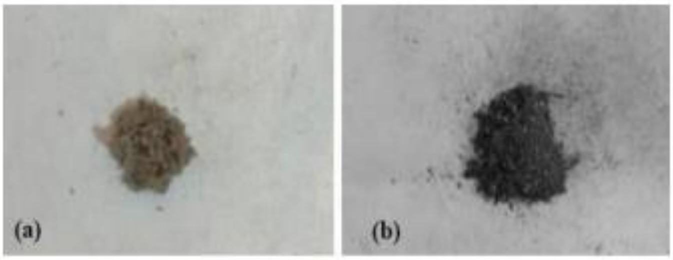

Figure 8 The powders of copper oxide (a) Without $CuCl_2$ and (b) With $CuCl_2$[21].

The adsorption of organic contaminants and the production of solar cells are only a few of the many uses for copper oxide nanoparticles. Using this approach to manufacture copper oxide for biomedical applications is a decent first step, and the results can be deemed satisfactory.

Figure 9 shows the transmission electron microscopy TEM image of the Ag nano-structures synthesized at (80 wt%) $AgNO_3$ and (20 wt%) sucrose with, preparation time of 25 min image a and b. The uniform, which is shaped similar (palm fronds), has been a grown-up and the smallest particle size was 20 nm. Whereas these shapes were vanished when the concentration becomes (60 wt% $AgNO_3$) and (40 wt%) sucrose at the same syntheses time 25 min, at that time, the Ag nanoparticles with minimum particles size was 10 nm as shown in Figure 9 (c) can be clearly comprehended. These results were assisted to employ the Ag nanoparticles for killing/sterilizing some types of bacteria.

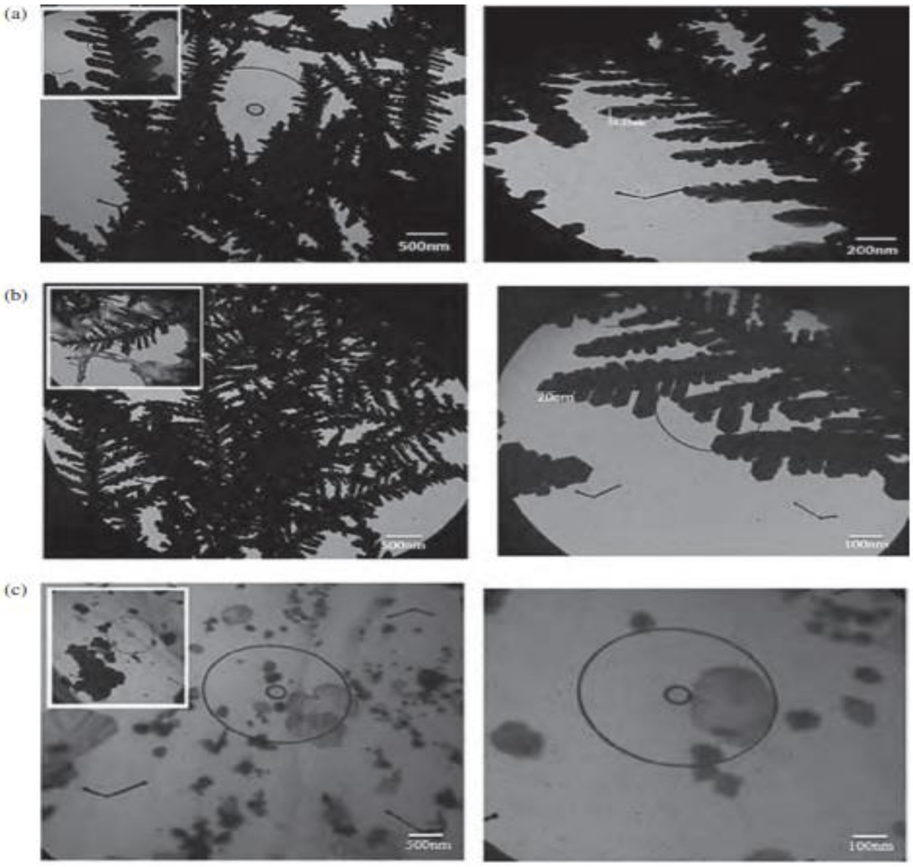

Figure 9. TEM images of AgNPs prepared at different ratio of $AgNO_3$ with different preparation time

Figure 10 shows the antibacterial activity of silver nanoparticles AgNPs. It was a perfect inhibition zone after a 24-hour incubation at 37 ºC in the plate. It was a good result to get the susceptible of strains to Ag nano-particles that display a large inhibiting zone, of two kinds of bacteria as shown in Table 1.

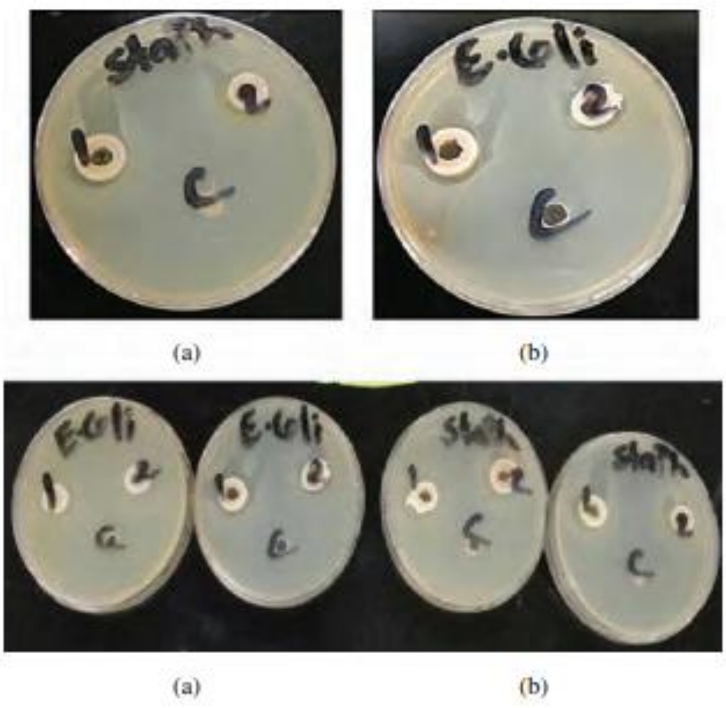

Figure 10. The bio-activity of (AgNPs): a- *Staphylococcus* and b *E.coli*.

Table 1. Inhibition zone in mm.

Sample No.	Control	Staphylococcus (mm)	Escherichia Coli (mm)
1	-	15	16
2	-	17	15
3	-	19	14
4	-	16	17

©SRP 2023, DOI: https://doi.org/10.47758/ijn.vi4.98

Conclusions

Numerous latest novel progresses prepared in a magnetron sputtering and atmospheric pressure plasma jet techniques were tackled in this review. It included the modification of both techniques in many several applications. Improvements in magnetron sputter and plasma jet sputtering have made it possible to produce critical tools for sterilization and decontamination in various environments. The products of some new essential studies in this review was correspondingly included in the preparation of nano-particles of copper oxide and a well-thought-out worthy challenge for killing/sterilizing bacteria/virus and detect toxic gases by using high novelty of copper oxide gas sensor. As a result, this study presents an overview of magnetron sputtering in the atmospheric–pressure plasma jet process, as well as highlighting the prospective applications of these techniques.

References

[1] Heinemann, M.; Eifert, B.; Heiliger, C. Band structure and phase stability of the copper oxides Cu2O, CuO, and Cu4O3 . Phys. Rev. B 2013, 87, 115111.

[2] Liu, A.; Nie, S.; Liu, G.; Zhu, H.; Zhu, C.; Shin, B.; Fortunato, E.; Martins, R.; Shan, F. In situ one-step synthesis of p-type copper oxide for lowtemperature, solution-processed thin-film transistors. J. Mater. Chem. C 2017, 5, 2524–2530

[3] Matsuzaki, K.; Nomura, K.; Yanagi, H.; Kamiya, T.; Hirano, M.; Hosono, H. Epitaxial growth of high mobility Cu2O thin films and application to pchannel thin film transistor. Appl. Phys. Lett. 2008, 93, 202107.

[4] Subramaniyan, A.; Perkins, J.D.; O'Hayre, R.P.; Lany, S.; Stevanovic, V.; Ginley, D.S.; Andriy, D.Z. Non-equilibrium deposition of phase pure Cu2O thin films at reduced growth temperature. Appl. Mater. 2014, 2, 022105.

[5] Wang, Y.; Ghanbaja, J.; Soldera, F.; Migot, S.; Boulet, P.; Horwat, D.; Mücklich, F.; Pierson, J.F. Tuning the structure and preferred orientation in reactively sputtered copper oxide thin films. Appl. Surf. Sci. 2015, 335, 85–91.

[6] Wang, Y.; Miska, P.; Pilloud, D.; Horwat, D.; Mucklich, F.; Pierson, J.F. Transmittance enhancement and optical band gap widening of Cu2O thin films after air annealing. J. Appl. Phys. 2014, 115, 073505.

[7] Moharam, M.M.; Elsayed, E.M.; Nino, J.C.; Abou-Shahba, R.M.; Rashad, M.M. Potentiostatic deposition of Cu2O films as p-type transparent conductors at room temperature. Thin Solid Films 2016, 616, 760–766.

[8] Dolai, S.; Das, S.; Hussain, S.; Bhar, R.; Pal, A.K. Cuprous oxide (Cu2O) thin films prepared by reactive d.c. sputtering technique. Vacuum 2017, 141, 296–306

[9] Alajlani, Y.; Placido, F.; Barlow, A.; Chu, H.O.; Song, S.; Rahman, S.U.; Bold, R.D.; Gibson, D. Characterisation of Cu2O, Cu4O3 , and CuO mixed phase thin films produced by microwave-activated reactive sputtering. Vacuum 2017, 144, 217–228.

[10] Akaltun, Y. Effect of thickness on the structural and optical properties of CuO thin films grown by successive ionic layer adsorption and reaction. Thin Solid Films 2015, 594, 30–34.

[11] Tripathi, T.S.; Terasaki, I.; Karppinen, M. Anomalous thickness-dependent optical energy gap of ALD-grown ultra-thin CuO films. J. Phys. Condens. Matter 2016, 28, 475801.

[12] Li, A.; Song, H.; Wan, W.; Zhou, J.; Chen, X. Copper oxide nanowire arrays synthesized by in-situ thermal oxidation as an anode material for lithiumion batteries. Electrochim. Acta 2014, 132, 42–48.

©SRP 2023, DOI: https://doi.org/10.47758/ijn.vi4.98

[13] Pattanasattayavong, P.; Thomas, S.; Adamopoulos, G.; Mclachlan, M.A.; Anthopoulos, T.D. P-channel thin-film transistors based on spray-coated Cu2O films. Appl. Phys. Lett. 2013, 102, 163505.

[14] Kawwam, M.; Alharbi, F.H.; Kayed, T.; Aldwayyan, A.; Alyamani, A.; Tabet, N.; Lebbou, K. Characterization of CuO(1 1 1)/MgO(1 0 0) films grown under two different PLD backgrounds. Appl. Surf. Sci. 2013, 276, 7–12.

[15] Liau, C.K.; Jhan, J.L. Investigation of rapid thermal annealing on Cu2O properties and n-p Cu2O homojunction performance by electrochemical deposition processing. J. Electrochem. Soc. 2016, 163, D787–D793.

[16] Rydosz, A.; Ziabka, M.; Michon, D.; Kanak, J.; Maziarz, W.; Pisarkiewicz, T. Gas Sensing Characteristics of MoO3 Thin Films Prepared by Glancing Angle Magnetron Sputtering. Sens. Lett. 2017, 15, 1–8.

[17] Chen, H.-I.; Hsiao, C.-Y.; Chen, W.-C.; Chang, C.-H.; Chou, T.-C.; Liu, I.P.; Lin, K.W.; Liu, W.-C. Characteristics of a Pt/NiO thin film-based ammonia gas sensor. Sens. Actuators B 2018, 256, 962–967.

[18] Y. Dai, et al., High-Surface-Area Mesoporous Crystalline TiO2: Synthesis, Characterization, and Application as Support for Making Stable Au Catalysts, Journal of Nanoscience and Nanotechnology 17 (6) (2017) 3772 Snyders, R.; Dauchot, J.-P.; Hecq, M. Synthesis of Metal Oxide Thin Films by Reactive Magnetron Sputtering in Ar/O2 Mixtures: An Experimental Study of the Chemical Mechanisms. Plasma Process. Polym. 2007, 4, 113– 126.–3778.

[19] Nafarizal, N. Precise Control of Metal Oxide Thin Films Deposition in Magnetron Sputtering Plasmas for High Performance Sensing Devices Fabrication. Procedia Chem. 2016, 20, 93–97. 20. Wang W, Varghese O K, Ruan C, Paulose M and Grimes C A 2003 J. Mater. Res. 18 2756,

[20] Basima Saleem Dawood , Ahmed Abed Anber , Eidan Asi Abdullah, FABRICATION OF NANOSTRUCTURED COPPER OXIDE THIN FILMS VIA HOME-MADE DC MAGNETRON SPUTTERING FOR GAS SENSING APPLICATIONS, Turkish Journal of Physiotherapy and Rehabilitation; 32(3), ISSN 2651-4451 | e-ISSN 2651-446X.

[21] Sarah Ahmed Hassan, Ahmed Abed Anber, Eidan Asi Abdullah, Jafer Fahdel Odah, Najwa J. Jubier , Ali Adnan Abd Alwahab " Electrical Properties and Optimum Conditions of A Home-Made Magnetron Plasma Sputtering System" Iraqi Journal of Science, 2021, Vol. 62, No. 11(Special Issue), pp: 4353-4363.

[22] Ahmed A Anber et al. (2018). ''Preparation of Nanoparticles Copper Oxide using an Atmospheric-Pressure Plasma Jet'', J. Phys.: Conf. Ser. 1032 012009.

[23] Ahmed Abed Anber1, Mohammed Shalan Essa, Ghada Ayad Kadhim, Ali Jabar Fraih, Adil A. Anber, Farqad F. Edin, Ammar S. Hameed, "Fabrication of Nanostructured Silver Liquid by Atmospheric-Pressure Plasma Jet for Bacteriological Applications" Journal of Bionanoscience Vol.12, 06, 809–813, 2018

[23]C.A.D.Santos, A.F. Jozala, A.P.Jr and M.M.Seckler. (2012). Journal of Nanobiotechnology. 10,43.

[24]Y.T.Zhang, Y.Guo, M.A.T.Cai. (2011). Chin.Phys.Lett. 28, 11.

[25]M.B.Ahmad, M.Y.Tay, K.Shameli, M.Z.Husssein and J.J. Lim. Int. J. Mol. Sci.12,(2011).

[26]Ahmed A Anber et al Fabrication of Nanostructured silver liquid by Atmospheric-Pressure Plasma Jet for Bacteriological Applications, 2018 Bionanoscience journal.

[27]Benson, H.J. (2002). Microbiological Applications Laboratory manual in General Microbiology. 8t h ed. McGraw-Hi l l . New York.

[28]Tankeshwar, A. (2015). API 20E Test System: Introduction, Procedure Results and Interpretations. Microbeonline.

©SRP 2023, DOI: https://doi.org/10.47758/ijn.vi4.98